CO_2 Laser Ablation Area Scaling And Redeposition On Flat Polyoxymethylene Targets

John E. Sinko[a], Stefan Scharring[b], Yosuke Tsukiyama[c], Katsuhiro Ichihashi[d], Naoya Ogita[d], Akihiro Sasoh[d], Noritsugu Umehara[c], Hans-Albert Eckel[b], and Hans-Peter Röser[e]

[a]*Micro-Nano Global Center of Excellence, Graduate School of Engineering, Nagoya University, Furo-cho, Chikusa-ku, Nagoya, Aichi, Japan 464-8603*
[b]*German Aerospace Center (DLR) – Institute of Technical Physics, Pfaffenwaldring 38 – 40, 70569 Stuttgart, Germany*
[c]*Department of Mechanical Science and Engineering, Nagoya University, Furo-cho, Chikusa-ku, Nagoya, Aichi, Japan 464-8603*
[d]*Department of Aerospace Engineering, Nagoya University, Furo-cho, Chikusa-ku, Nagoya, Aichi, Japan 464-8603*
[e]*Institute of Space Systems (IRS), University of Stuttgart, Pfaffenwaldring 31, 70569 Stuttgart, Germany*

Abstract. One of the remaining unknown subjects of laser propulsion involves whether special benefits or challenges exist for applying laser ablation propulsion to targets with particularly large or small spot areas. This subject is of high importance for a wide range of topics ranging from laser removal of space debris to micropropulsion for laser propulsion vehicles. Analysis is complex since different ablation phenomena are dominant between atmosphere and vacuum conditions. Progress has also been impeded by the difficulty of setting control parameters (particularly fluence) constant while the spot area is adjusted. It is also usually difficult for one group to address small- and large-area effects using a single high-power laser system. Recent collaborative experiments on laser ablation area scaling at several institutions, using 100-J class and 10-J class CO_2 lasers, have advanced the understanding of laser propulsion area scaling. The spot area-dependence of laser propulsion parameters has been investigated over an area range covering approximately 0.05-50 cm^2 at low fluence of about 0.6 J/cm^2. The experiments were conducted well below the threshold for plasma formation, and provide an estimate of the ablation threshold for CO_2 laser ablation of POM.

Keywords: Laser propulsion, CO_2 laser, redeposition, polyoxymethylene, profilometry
PACS: 07.60.Pb, 41.75.Jv, 61.72.S-, 61.80.Ba, 79.20.Ap, 79.20.Eb, 81.15.-z, 81.70.Jb

INTRODUCTION

Theoretical Overview

Several works in the literature [1-6] have discussed the subject of area scaling as it relates to laser propulsion, as well as the physical phenomena underlying any hypothetical scaling effects. For example, area-dependence could be a result of thermal diffusion, diffraction, rarefaction waves, redeposition, or radiative exhaust. This paper will expand on the understanding of area-dependence and examine some additional results for this topic. In doing so, we will use the ablated mass *m*, the

CP1278, *International Symposium on High Power Laser Ablation 2010,* edited by C. R. Phipps

momentum coupling coefficient C_m, and the characteristic laser spot area a. C_m is defined as follows:

$$C_m = \frac{I}{E} = \frac{\sigma}{\Phi}, \quad (1)$$

where E is the laser pulse energy, I is the imparted impulse, σ is the area-density of impulse and Φ is the fluence of the laser beam at the target surface ($\Phi = E/a$). It must be noted that we will treat Φ as an average, representative quantity for simplicity; in reality, the fluence can vary significantly between various points within the beam.

We also wish to consider the effect of exhaust dimensionality. The exhaust undergoes nearly 1-dimensional expansion in the case of large spot area (*i.e.*, edge effects are minimized). In this case, the first moment of the exhaust velocity may be specified as v_z. In a sense, v_z represents the ideal net exhaust velocity, an upper limit of possible exhaust velocities. If we instead consider an isoenergetic, fully radial expansion, such as would be the case for a very small, point-like spot area, the first moment in the z-direction is only ½ v_z. In reality, neither of these cases is absolutely correct when applied to laser ablation, but the net velocity will be somewhere in between these extreme limits during ablation of flat surfaces. If the same mass is removed in both cases, then considering imparted impulse, we would expect inefficiency to be introduced in ablation at small spot areas due to the nonlinear nature of the exhaust and enhanced significance of edge behavior. It remains to be seen what physical range of spot areas these effects describe.

Other effects on area scaling may arise from redeposition. The redeposited layer might skew the measured ablated mass; and also, from a consideration of conservation of momentum, if the material has sufficient (reverse) velocity to affect the net impulse when it is redeposited, it could reduce the total imparted impulse. By 'reverse velocity' we mean that any particles in the plume which impact the target surface must be traveling in the direction of the surface, rather than away from it. Even if the redeposited mass is insignificant, the impulse might not be. From a laboratory perspective, it has been challenging to address this issue, since any redeposited mass will be measured on the balance along with the ablated sample. Approaches involving removal of the redeposited material are difficult, as the ablation sample will generally be damaged in this case, and in any event, it is very difficult to ensure that the redeposited material was all removed. In this paper, the thickness of the redeposited layer will be tested using surface profilometry.

There are further considerations. Even if the redeposited layer does not significantly affect the total ablated mass, or the imparted impulse, it may still affect the reflectivity of the surface and the effective absorption coefficient of the target on subsequent shots. The roughness of the redeposited layer (and of the underlying propellant material) is of considerable significance as it relates to the surface reflectivity. Within the ablation crater, assuming the laser beam is aimed at a constant position on the target, we may expect that the redeposited layer is generally very thin, because at each shot, the layer is ablated along with the underlying target material. However, if the sample surface is large, other portions of the target may be masked by such redeposited debris after many shots. This issue is pertinent in both vacuum and air conditions, and is an important consideration for laser propulsion engines from the

standpoint of fouling. Specifically, there may be a need for protection of the engine and/or optics components from contamination by redeposited exhaust.

Notes about this Collaborative Study

This experimental investigation of area scaling builds upon work conducted at the University of Alabama in Huntsville (UAH) and Nagoya University (NU). Tests at UAH were preliminary in nature, and those at NU were limited by the laser pulse energy (~10 J) of the industrial CO_2 laser used at the facility. For a fluence of 0.6 J/cm^2, a spot area of about 5 cm^2 area (after shaping the beam) was possible at NU; for a fluence of 20 J/cm^2, the maximum spot area was around 0.5 cm^2. A recent collaboration between Nagoya University (NU) and the German Aerospace Center (Deutsches Zentrum für Luft und Raumfahrt, DLR), in part, sought to extend the upper limits of investigation by about an order of magnitude. The collaboration has also addressed topics related to laser ablation measurements and standardization [7,8]. The electron beam-sustained laser at DLR had a maximum output of around 150 J, more than an order larger than the beam at NU, allowing a much wider range of areas to be studied. This was a natural opportunity for collaborative research. A subset of the NU results was previously presented in [5], and have been supplemented here with additional results for a more thorough and complete presentation of the dataset.

Experimental Techniques

At NU, a TEA CO_2 laser (Selective Laser Coating Removal GmbH, model ML205E) was operated at up to about 10 J pulse energy to ablate cylindrical polyoxymethylene (POM) targets (diameter ϕ=25.8mm × thickness t=10mm). The targets were in a manufactured state characterized by surface variations in 2-dimensions notated as x (short period) and y (long period), which were visible to the naked eye. Surface profilometry and tribology experiments were conducted in collaboration between the Sasoh and Umehara laboratories at NU using a mechanical surface profilometer (Mitsutoyo SurfTest SV-3100). The aforementioned supplier processing pattern was not generally evident in the x-direction during the profilometric analysis; nevertheless, a roughness of about 500 nm was observed in this direction. In the y-direction, the mechanical processing pattern had a period of about 750 μm and average variation of 1-2.5 μm, generally overlaid onto the same magnitude of roughness (~500 nm) as in the x-direction. In addition to these measures, the POM area scaling targets at NU were processed to 3000 grit using a lapidary polisher (Maruto Doctor-Lap). An optical microscope (Olympus Optical Co., Ltd. BX60MF5) and 3-CCD color camera (Olympus U-SPT in combination with Olympus Japan CS580 and Olympus PMTVC) were also used in the research. Laser pulse energy was measured by a 50 × 50 mm thermopile energy detector (Gentec QE50LP-H-MB-DO) and the temporal pulse profile was measured by a photon drag detector (Hamamatsu B749). Piezoelectric force sensors (PCB Piezoelectronics, Inc. model 208C01) were used to measure total imparted impulse. Mass was measured with a scientific balance (Shimadzu Corporation AW320) with 0.1 mg readability, but the general accuracy of the device is a little larger, about ±0.3 mg.

Laser ablation experiments at DLR were conducted using a custom electron beam-sustained CO_2 laser with up to about 150 J pulse energy to ablate plate homopolymer POM targets (200mm × 200mm × t=5mm). At DLR, laser pulse energy was measured by a ϕ=46mm thermopile energy meter (Ophir PE50BB-SH-V2) and the pulse profile was measured by a photoelectromagnetic IR detector (Vigo Systems S.A., PEM-L-3). Impulse was measured by piezoelectric force sensors (PCB Piezoelectronics, Inc., models 208C01, 208C04, and 200C20). Mass was measured using a scientific balance (PCE group LS-500) with 1 mg readability, but in fact the measurement accuracy for this instrument was closer to 3 mg, a point which caused some difficulty during the experimental measurements in this study. It may be noted that a more sensitive balance was used for the data taken at UAH (Mettler AE163, 0.01 μg readability, ~0.03 μg accuracy). The balances at UAH and NU were both aided by enclosed glass walls for thermal and aerodynamic isolation from the laboratory environment. The DLR balance had a circular plate fitted with a ~10 cm tall, clear plastic case for sample isolation, but this could not be used during the experiments, due to the large size of the square targets, which did not entirely fit under the case.

RESULTS

Ablative Impulse and Mass Removal Results

The results for the area scaling tests made at NU and DLR are shown below in Figures 1 and 2 along with a comparable result previously reported by UAH [6].

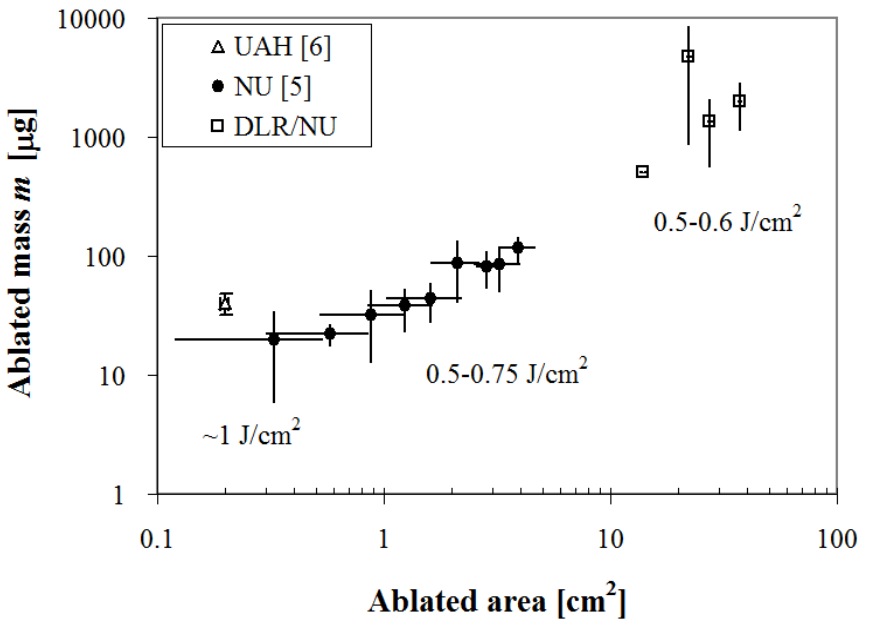

FIGURE 1. Area scaling results at 101 kPa for ablated mass m

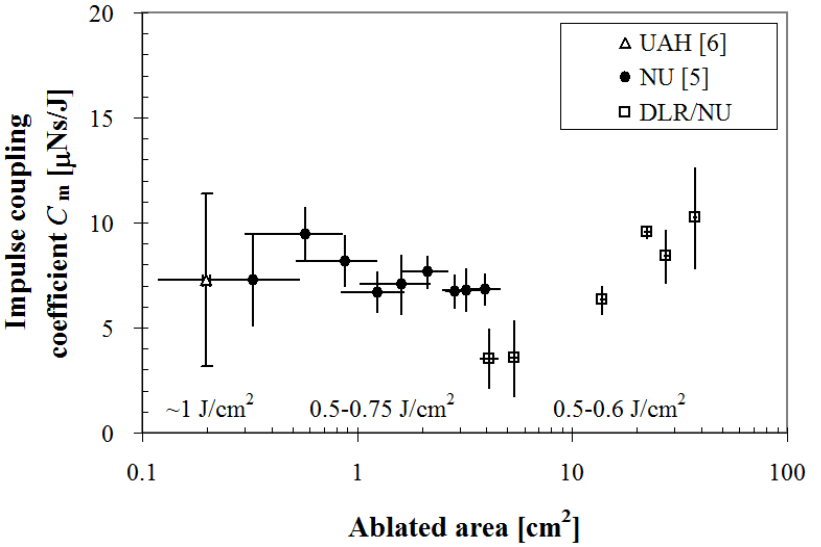

FIGURE 2. Area scaling results at 101 kPa for momentum coupling coefficient C_m

The results for both m and C_m suggest that in air near the ablation threshold, there is no significant area scaling effect. It may be noted that experiments around the critical ablation threshold (~0.5-1 J/cm^2) must be carefully set up, due to the relative sensitivity of the coupling coefficient to changes in fluence within this regime.

CFD Modeling Results

A 2-dimensional computational fluid dynamics (CFD) model, developed by Ichihashi and Sakai [9] at NU, was used to explore the effect from laser ablation at different spot areas, both in terms of the flow-field and of the ablated crater. In the flow-field, we believe that the dimensionality of the exhaust strongly affects the momentum coupling coefficient. Of particular interest are the limits of 1-dimensional exhaust (at large spot area), 3-dimensional exhaust (meaning fully radial, '1-dimensional' expansion from a point) and the regime between these extremes. The spot areas we used in experiments were limited on the small side by lack of sufficiently fine, precise techniques (specifically, diagnostics for mass and impulse), and on the large side by lack of sufficiently powerful equipment (meaning high-power lasers). Although the CFD model is not bounded by these practical limitations, we believed it was most appropriate to advance modeling only as far as experiments.

The flow-field (in terms of velocity contours) is shown in Figure 3. The dark areas in Fig. 3 indicate higher velocities. A very significant difference is evident between the 0.05 cm^2 and 50 cm^2 cases in the figure. As expected, the result for the 0.05 cm^2 case implies that the cross-section has almost circular expansion, whereas the 50 cm^2 case appears to be almost planar expansion. Based on the discussion in the introduction, this difference should have a significant effect on the total impulse

measured, about a factor of 0.5 in a '3-dimensional' treatment to 1 in a 1-dimensional treatment.

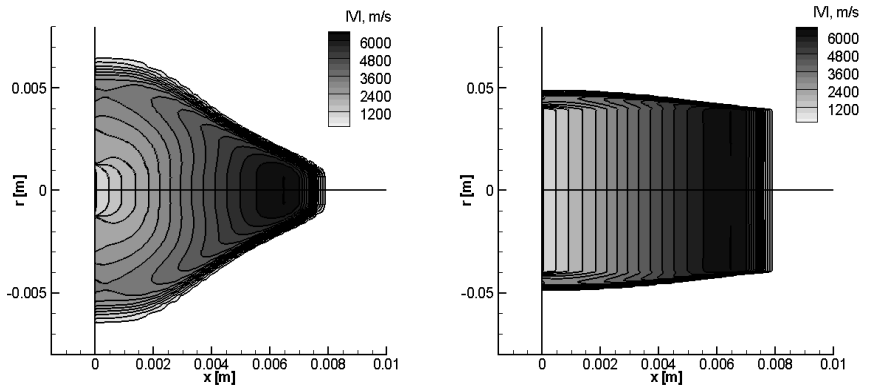

(a) **(b)**

FIGURE 3. CFD velocity contour flow-field predictions for (a) 0.05 cm^2 and (b) 50 cm^2 at 1 μs after the arrival of the laser pulse and 0.6 J/cm^2 fluence. *x* denotes distance from the target surface and *r* is a radial coordinate. The experiment used experimental data taken with the NU CO_2 laser to simulate the temporal profile of the laser pulse.

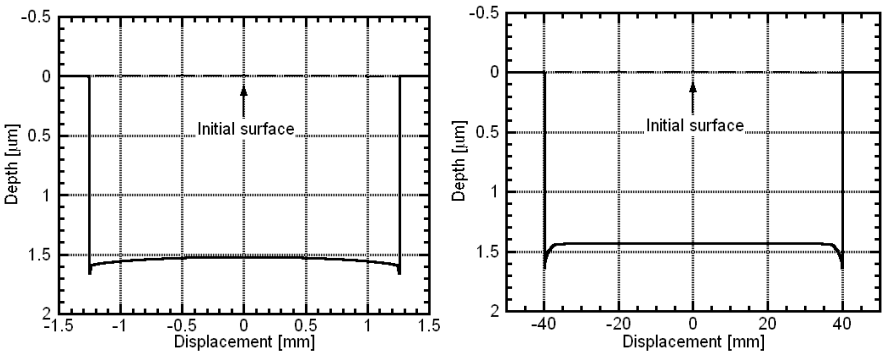

(a) **(b)**

FIGURE 4. CFD ablation crater predictions for (a) 0.05 cm^2 and (b) 50 cm^2 for 0.6 J/cm^2 fluence

The results in Fig. 4 show only small differences between the small- and large-spot area cases. Interestingly, the crater for small spot area is deeper than the one for large spot area. This result probably stems from the greater influence of the sharp ablation zone at the edge of the crater. In the 50 cm^2 spot area case, the crater is nearly flat, and the edge effect is almost negligible. In any event, the difference between the small- and large-spot area cases is still small relative to the total crater depth, indicating that even in this extreme case (3 orders of magnitude difference in areas), there is little effect on the ablated mass as the spot area changes near the threshold fluence.

Profilometry and Optical Microscopy Results

Since area scaling is strongly dependent on the surface condition of the target, an in-depth surface analysis of the POM samples was conducted in collaboration with the Umehara lab at NU. Optical microscopy of the crater edges was used to study redeposition of particles around the ablation craters. Typical results are shown in Figures 5 and 6 for samples ablated at similar fluences, around 1 J/cm^2.

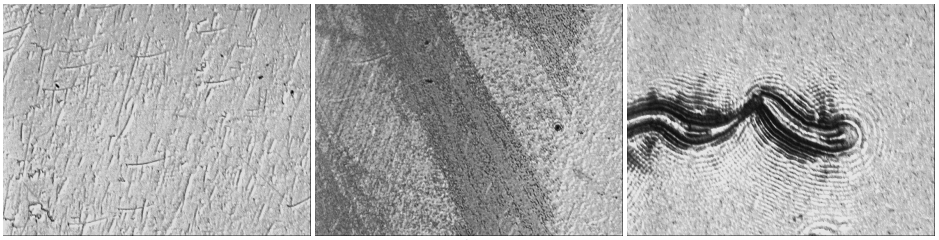

(a) (b) (c)

FIGURE 5. Optical microscopy of DLR plate target A9, ablated at DLR-Stuttgart, Germany under ≈1 J/cm^2 fluence; (a) unablated surface (b) redeposition on unablated surface, around the ablation crater, (c) ablated surface, including diffraction bands generated around a debris fiber. Each image is 1 mm wide.

In Figure 5(a), The unablated surface is seen to include either fibrous material or molded striations of POM. The redeposited material in Figure 5(b) covers this surface. During the transportation of this sample from Germany to Japan for profilometry analysis, some of the redeposited material appears to have been removed, possibly through abrasive contact with the plastic bag in which it was stored. The samples at DLR were ablated in atmospheric conditions, and some small amount of debris were present, such as the fiber in Figure 5(c), in the center of the ablation crater. The presence of such material is noted for completeness; tests at NU indicate that an unprepared surface has about 1 order of magnitude higher variance in impulse than a surface prepared by shooting several 'cleaning shots' at low fluence (in the case of CO_2 ablation of POM, ≈0.2 J/cm^2). Ablation of a target of the same type was performed at NU (with cleaning shots) in order to compare ablation threshold data; the results are shown below in Figure 6.

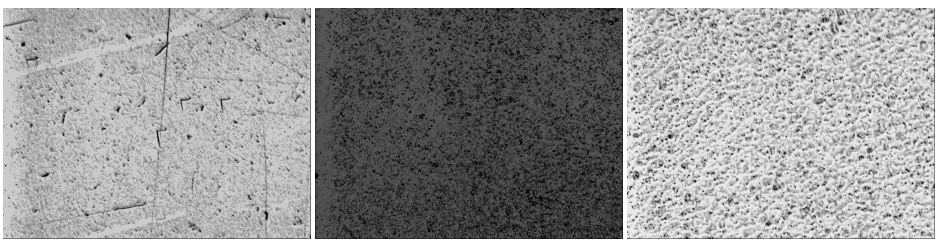

(a) (b) (c)

FIGURE 6. Optical microscopy of DLR plate target "B", ablated at NU, Japan under ≈1 J/cm^2 fluence; (a) unablated surface, (b) redeposition on the unablated surface around the crater, (c) ablated surface in the center of the crater; most debris was removed before ablation by 10 'cleaning shots' at 0.2 J/cm^2. Each image is 1 mm wide.

The microscopic photograph in Fig. 6(a) shows typical features of unablated surfaces. Fig. 6(b) shows the redeposited area around the crater, and Fig. 6(c) shows the crater center, wherein the ablation of the surface appears to have generated a fine pattern of tiny craters and ridges. It is unclear whether the scale and positions of these features correspond to speckle in the laser beam or merely chaotic hydro- or thermodynamic phenomena. Redeposition usually produces a well-delineated ring around the ablation crater, as shown in Figure 7 for an ablation experiment on 8/12/2009 at ≈2 J/cm^2 (pulse energy 1.90±0.01 J) following 10 successive shots at the target.

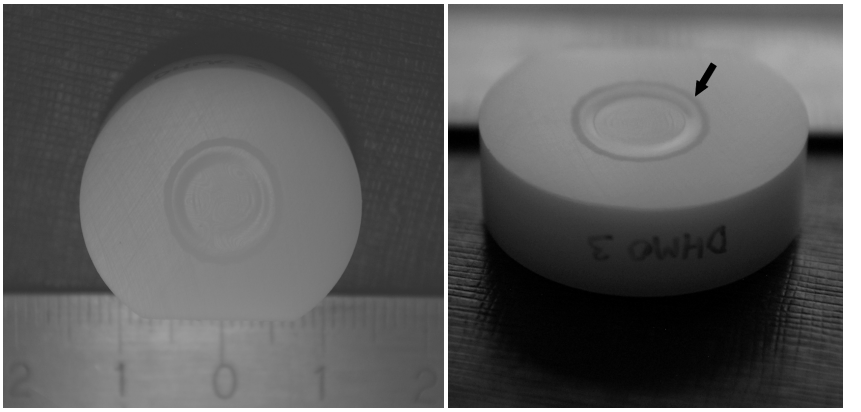

(a) (b)

FIGURE 7. 8/12/2009, laser ablation redeposition around crater: (a) top view, (b) oblique view; the redeposition region, indicated by an arrow, has total width ≈750 μm as measured from the image in (a).

The ring is darker (indicating higher optical absorption or diffuse reflectivity) than the surrounding surface, even at low fluence ≈1 J/cm^2. Thus, the thickness of redeposited material is of interest, in case enough material is redeposited to affect imparted impulse or the infrared absorptive and reflective properties of the surface. The thickness can be directly estimated using surface profilometry. Fig. 8 shows the profilometry analysis on the crater from Fig. 7 (scans were made parallel to the flat, truncated side of the target). The depth of redeposition, *at most* about 500 nm, as shown in Fig. 8(b), is insignificant compared to the total crater depth (≈70 μm), which is strong evidence that redeposition does not directly affect ablated mass or imparted impulse during laser ablation. However, the optical microscopy results suggest that the redeposited material may still affect subsequent ablation due to changes in the absorption coefficient and surface reflectivity. The surface roughness may affect the total reflectivity due to the introduction of diffuse reflectivity components. For instance, the roughness (standard deviation) from 13 to 13.5 mm displacement in Fig. 8 is about ±190 nm for the unablated surface (which had been polished to 3000 grit) and about ±510 nm for the ablated surface. Although the roughness should be important for ablation at lower wavelengths (e.g., Nd:YAG laser ablation), the variation is still about an order of magnitude less than the laser wavelength, indicating that reflectivity effects should be minimal.

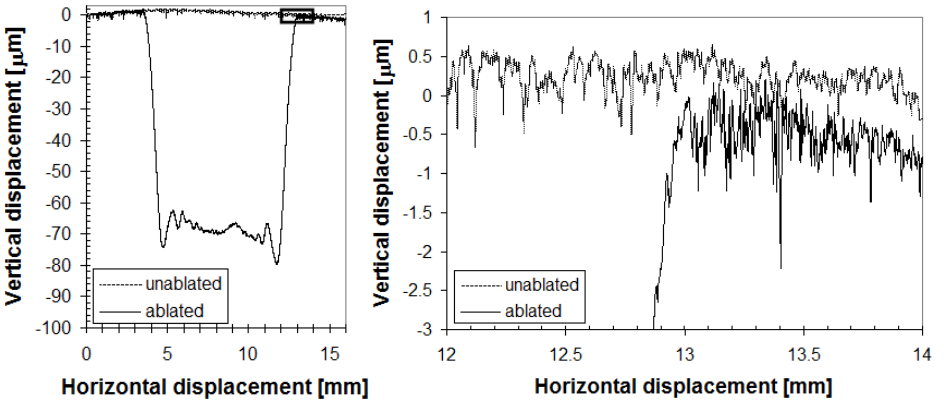

FIGURE 8. Profilometry scans of POM target before (dotted line) and after (solid line) ablation at ≈2 J/cm^2 fluence, (a) showing the entire crater and (b) the right edge of the ablation crater in a region where redeposition was observed; (b) shows the area in (a) within the small box at upper right. The absolute z-positions of the traces were arbitrarily adjusted for clarity.

That leaves only absorption as having a possible effect on subsequent ablation. The composition of the redeposited material is therefore of interest. For CO_2 ablation, which probably occurs via a vibrational/thermal pathway, redeposition is expected to include a significant amount of carbon, based on numerical studies by Andre [10] of electrical ablation of POM. Under this interpretation, redeposition comes from the relatively low-temperature (less than about 1500 K) condensation of solid carbon (e.g., graphite) from the ablation plume onto the cooler surrounding surface. Compared to other polymers studied in [10], less carbon is produced in the ablation exhaust from POM. We would therefore expect carbon redeposition only within a narrow regime in which the exhaust is sufficiently hot, and the surface sufficiently cool, to support the redeposition process. These results are consistent with our findings; namely, thin, sharply-defined rings of dark, redeposited material around ablation craters in POM. For further confirmation of the composition of redeposited material, an ATR-FTIR study of the surface is planned.

CONCLUSIONS

Experiments on area scaling near the ablation threshold of polyoxymethylene were conducted at DLR and NU, and compared to a similar measurement reported by UAH. Area scaling near the ablation threshold, in atmospheric conditions, was found to have little to no effect on ablation despite testing across a wide range of spot areas (about 3 orders of magnitude).

CFD results generally support the findings, but predict that at sufficiently small spot area, the net imparted impulse should be reduced compared to large spot areas, based on the dimensionality of the plume, a fact supported by analytical consideration. However, the experimental area regimes in which these effects may be found remain unclear.

Surface profilometry and optical microscopy were used to investigate redeposition effects during CO_2 laser ablation of POM. The results indicate that the redeposited material, of some hundreds of nanometers depth, is insufficient to directly affect the imparted impulse or ablated mass. Profilometry reveals that the roughness of the redeposited region is probably insufficient to cause any significant surface reflectivity effects at 10.6 μm wavelength. However, optical microscopy observations suggest that the redeposited material may measurably influence the absorption coefficient of the target, an effect which *could* affect the target behavior at 10.6 μm in subsequent shots. Based on other POM ablation literature, the probable major component of the redeposited material is carbon, but an ATR-FTIR study of the surface is planned for confirmation.

ACKNOWLEDGMENTS

The authors gratefully acknowledge financial support from a Micro-Nano Global Center of Excellence Young Researcher Award. In addition, Nagoya University, the Micro-Nano Global Center of Excellence, and DLR-Stuttgart supported this study.

REFERENCES

1. J. P. Reilly, A. Ballantyne and J. A. Woodroffe, *AIAA J.* **17**(10), 1098-1105 (1979).
2. J. E. Sinko, "Constant-Fluence Area Scaling for Laser Propulsion" in *Fifth International Symposium on Beamed Energy Propulsion*, edited by A. V. Pakhomov, AIP Conference Proceedings 997, American Institute of Physics, Melville, NY, 2008, pp. 242-253.
3. J. E. Sinko, "Shock wave and vapor plume measurements for area scaling in laser propulsion" in *Symposium on Shock Waves in Japan*, Nagoya University, Nagoya, Japan, 2009, pp. 299-302.
4. J. E. Sinko, "Measurements of shock waves produced by TEA CO_2 laser ablation in atmospheric conditions" in *Symposium on Shock Waves in Japan*, Nagoya University, Nagoya, Japan, 2009, pp. 291-292.
5. J. E. Sinko, "CO_2 Laser Ablation Propulsion Area Scaling with Polyoxymethylene Propellant" in *Sixth International Symposium on Beamed Energy Propulsion*, edited by C. R. Phipps, K. Komurasaki and J. E. Sinko, AIP Conference Proceedings, American Institute of Physics, Melville, NY, to be published 2010
6. J. E. Sinko, "Vaporization and Shock Wave Dynamics for Impulse Generation in Laser Propulsion", Ph.D. Thesis, The University of Alabama in Huntsville, 2008.
7. J. E. Sinko, S. Scharring, H.-A. Eckel, H.-P. Röser, and A. Sasoh, "Measurement Issues in Pulsed Laser Propulsion" in *Sixth International Symposium on Beamed Energy Propulsion*, edited by C. R. Phipps, K. Komurasaki and J. E. Sinko, AIP Conference Proceedings, American Institute of Physics, Melville, NY, to be published 2010
8. S. Scharring, H.-A. Eckel, H.-P. Röser, J. E. Sinko, and A. Sasoh, "Laser Propulsion Standardization Issues", these proceedings.
9. K. Ichihashi, "Calculation of Impulse Generated by Pulse Laser Ablation on Polyacetal" in *27th International Symposium on Space Technology and Science*, ISTS Conference Proceedings, 2009, Paper 2009-b-29s.
10. P. André, *J. Phys. D: Appl. Phys.* **30**, 475-493 (1997).